International Journal of Scientific & Engineering Research, Volume 10, Issue 8, August-2019
ISSN 2229-5518

Local Scour Around Bridge Abutment

Aya M. Elkhouly, Mohamed T. Shamaa Tharwat A. Sarhan, Riham M. Ezzeldin

Abstract— A group of laboratory experiments were conducted to evaluate the maximum scour depth around various abutment shapes. In this research a comparison between different shapes of abutment were carried out as vertical abutment, semicircular ended abutment, abutment with vertical sloped face, and wing wall abutment. Also, the influence of pile existence to reduce the maximum scour depth was investigated. For vertical abutment, it was observed that the width change affect slightly on the scour depth. For semicircular ended abutment, the increase of the radius of curvature (R) leads to decrease scour depth. In case of abutment with vertical sloped face, it was proved that the increase of side slope angel (θ) leads to reduce scour depth. For wing wall abutment, it was proved that the decrease of wall angel (∝) leads to reduce scour depth. The results indicated that wing wall abutment with $\propto = 60°$ gave the minimum scour depth compared with the other studied abutment shapes. It minimized the maximum scour depth by 22.68% compared with vertical abutment. Also pile existence with *($D_p/B=0.08$, $X/B=0.25$)* reduced the maximum scour depth by 22% compared with no pile case. For all abutment shapes when the Froude number increases the maximum scour depth increases. Empirical relations were derived to predict the maximum scour depth for the studied types of abutment shapes.

Index Terms— Abutment, Scour, Vertical abutment, Semicircular ended abutment, Vertical abutment with sloped face, Wing Wall abutment, Piles.

1 Introduction

Bridges are important links in our nation's infrastructure that must be protected in order to provide safety and serviceability for the public. Bridges play an important role in cultural, social and economic improvement [1]. Throughout history, catastrophic bridge failures have occurred resulting in the loss of human life, disruption of commerce, and enormous repair costs. Foundation, structural and hydraulic failures are the most possible reasons of the bridges collapse [2], [3] and [4].

Scour is a phenomenon caused by the erosive action of water in rivers and streams. As a result of flowing water, excavating and carrying away material from bed and banks of streams around the piers and abutments of bridges producing scour holes that affect the stability of the structure, cause reduction in strength of the foundation of a bridge and will undoubtedly result in its collapse. Safely designing of the bridge foundation needs an accurate estimation of scour depth. The hydraulic failures have been specified to be the most common type of bridges failure [5].

The various types of scour that can occur at a bridge crossing are typically referred to: general scour, contraction scour and local scour but local scour is the most critical one [6], [7] and [8]. Generally, local scour depths are much greater than general or contraction scour depths, often by a factor of ten [9]. Local scour is related to the sediment removal around bridge foundation, namely abutments, or piers, or piles [10]. It happens as a result of the flow velocity at the location of the bridge foundation due to the interaction between water and bridge foundations. This interaction results in vortices that cause a scour hole around bridge foundations as shown in Fig. (1). Also, existences of structures on the waterway increase the local flow velocities and turbulence level, so this can give rise to vortices that exert increased erosive forces on the adjacent bed and remove the sediment material in the surroundings of bridge piers or abutments [11]. The basic mechanism causing local scour at bridge abutments and piers is the formation of vortices at their base. The vortex removes bed material from the base of the obstruction. Scour hole develops when the sediment transport rate, which is outgoing from the scour hole is greater than that coming into the hole. When the scour depth increases, the strength of the vortices is reduced. Furthermore, there are vertical vortices downstream of the structure named wake vortices. The intensity of wake vortices decreases rapidly as the distance downstream of the structure increases.

A study done by The Federal Highway Administration of USA showed that 25% of the failures included piers damage while 75% occurred due to scour around abutments [12]. So One of the important issues in hydraulic engineering is inspection of local scour depth around bridge piers and abutments. Although scour rate may be greatly affected by the presence of structures encroaching on the channel, the shear stress generated by the water flow on the streambed is the basic erosive stress, while the streambed materials provide the resisting stress against erosion. Scour reaches its equilibrium status when these two stresses are balanced.

The existence of a pile upstream the bridge abutment reduces water collisions at the upstream face of the abutment and forces water to draw back to the bottom causing scour. If the abutment is found in the area of the dead zone behind the pile, it is important to investigate the diameter of pile and its distance from the abutment. Pile upstream the bridge abutment may cause positive or negative impact on the activity of soil particles movements around the abutment. The existence of pile causes a stagnant area works to reduce velocity and increase sedimentations in that area.

In this research, series of experiments were conducted to simulate the local scour around different models of proposed abutments' shapes in non-uniform sediment under clear water condition with v/v_c ratio ranges between 0.49

Aya M. Elkhouly is Researcher, Irrigation & Hydraulics Dept., Faculty of Engineering, Mansoura University, Egypt. E-mail: Aya.elkholi@gmail.com
Mohamed T. Shamaa is Associate Prof. of, Irrigation & Hydraulics Dept., Faculty of Engineering, Mansoura University, Egypt. E-mail: tarekshamaa@yahoo.com
Tharwat A. Sarhan is Associate Prof. of, Irrigation & Hydraulics Dept., Faculty of Engineering, Mansoura University, Egypt. E-mail: prof_tharwat@hotmail.com
Riham M. EzzEldin is Lecturer of, Irrigation & Hydraulics Dept., Faculty of Engineering, Mansoura University, Egypt. E-mail: eng_ezzeldin@hotmail.com

and 0.97. The main objective of this study is to find the abutment model which able to decrease the maximum scour depth. The focused points in the experimental results can be summarized as follows:

- The influence of Froude number on the maximum scour depth.
- The influence of the change of abutment shape on the maximum scour depth.
- The influence of pile existence on the maximum scour depth.

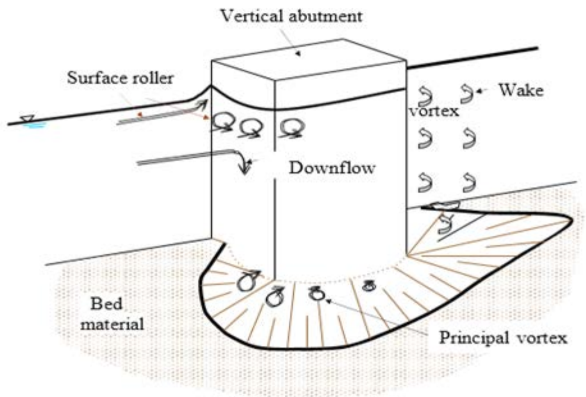

Fig. (1) General view of the abutment scour (after Graf.1996).

2 EXPEREMINTAL PROCEDURES

Experimental investigations were performed in a rectangular straight channel at the Laboratory of Hydraulic and Irrigation, Faculty of Engineering at Mansoura University, Egypt. This flume is 6.8m long, 0.74m wide and 0.4m height.

The flume has a closed-loop water system and supplied with water from underground water tank using a centrifugal pump. The pump conveys water to the approaching basin through the first and the second head water tanks. A tail gate is mounted to control the flow depths through the flume. To measure the flow discharge, a rectangular weir is installed at the entrance of the approaching basin. Moreover, an inlet screen filled with gravel has been installed at the downstream of the approaching basin to decrease the turbulence of water. The flume has a point gauge with vertical scale and Vernier. The measuring accuracy of the vertical scale in this point gauge is 0.1 mm. A sand trap is used at the end of the flume to prevent the sand movement to the underground tank. Before starting any experiment sand bed is prepared by using a preparing tool made of wood. The channel bed covered with a sand layer with 15 cm thickness. The median diameter of sand d_{50}=0.74 mm and the geometric standard deviation of particle size distribution ratio of σ_g = 2.08 mm. The general view of the channel is shown in Fig. (2).

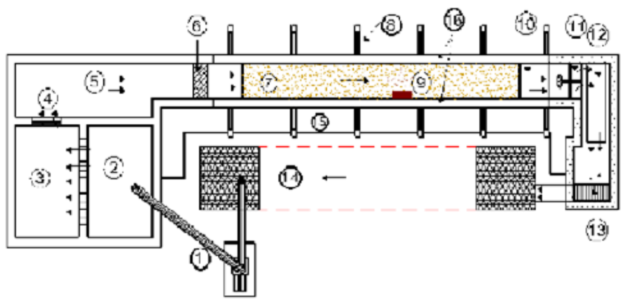

Fig. (2) Plan of the channel

The components of the channel shown in Fig. (2) are:

(1) Centrifugal pump	(9) Abutment model
(2) First head tank	(10) Sand trap
(3) Second head tank	(11) Tail gate
(4) Flow measuring weir	(12) Collecting tank
(5) Approach basin	(13) Graduated tank
(6) Inlet screen	(14) Laboratory sump
(7) Sand bed	(15) Side walk
(8) Wood bracing	(16) Rails for point gauge

At the beginning of the experimental work, many runs were carried out to determine the suitable discharge rates, water depths and runs duration. The preliminary tests were conducted for 7 hours with flow condition (Q = 20.976 lit/sec & Fr = 0.33520) to determine the maximum scour depth around the vertical abutment. The readings were taken every 20 minutes during this test. After four hours the scour depth does not appreciably increase with time. At six hours, moreover, the depth of scour does not change in comparison with its counterpart at seven hours. The difference between the scour depths after four hours and after seven hours is less than 1 mm as illustrated in Fig. (3). Thus, it can be considered that the equilibrium depth of scour occurs at four hours. Thus four hours was chosen as a test duration for all the experiments in this research.

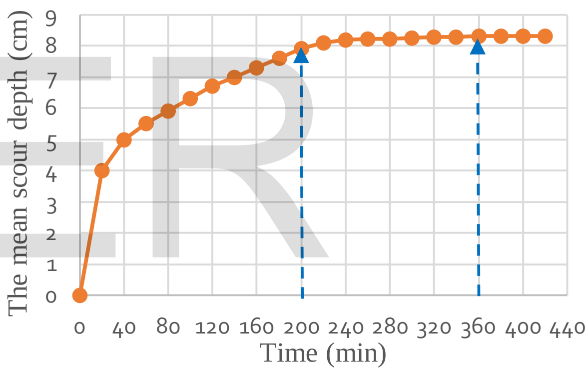

Fig. (3) The time development of scour depth with Fr = 0.33520

2.1 Abutment models

All abutments were made of wood and were painted with a varnish as a glue material to close its pores to avoid the water penetration. Abutments were placed vertically in the middle of the right wall of the channel. Also, abutments were placed with the orientation 0.0 degree to the flow direction.

In this research, five sets of abutments were used each set included three models with different flow conditions.

A. The first set

This set included three vertical abutments with different width as shown in fig. (4) to study the effect of abutment width (B) on the pattern and depths of scour. The abutment width used in this research were B= 3 cm, 5 cm and 10 cm.

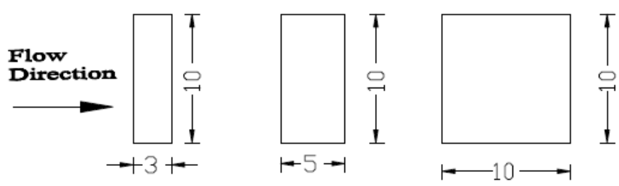

Fig. (4) Plan of the first set models

B. The second set

The second set included three semicircular ended abutments with different curvature radii of each abutment as shown in Fig. (5) to study the effect of the radius change (R) on the scour depth. The abutment radii used in this research were R= 1, 2, and 3 centimeters.

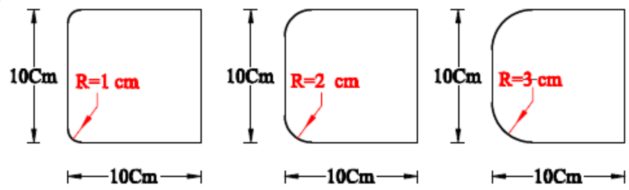

Fig. (5) Plan of the second set models

C. The third set

The set included three shapes of abutments with vertical sloped face as shown in fig. (6) to study the effect of the slope change (θ) on the scour depth. The abutment angle (θ) used in this research were θ = 10°, 15° and 20°. All lengths in the following figure are in centimeters.

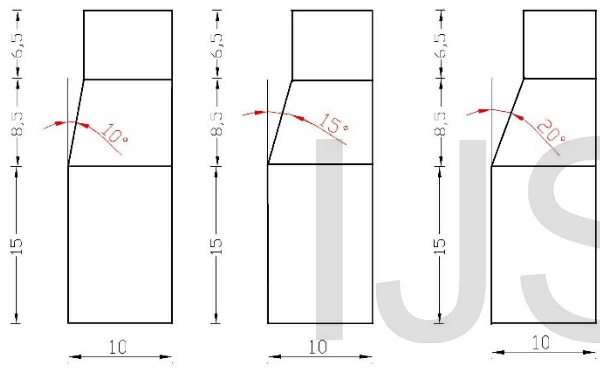

Fig. (6) Side view of the third set

D. The fourth set

The fourth set included three wing wall abutments with different wall angel α = 60°, 65° and 70° as shown in fig.(7). The effect of the wall angel (α) on the scour depth was studied and compared with the vertical wall abutment with angle α = 90°.

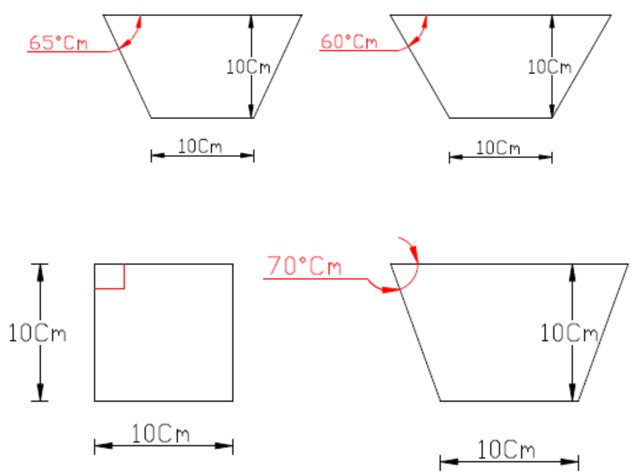

Fig. (7) Plan of the fourth set models

E. The fifth set

Vertical abutment and Sacrifice piles were used in this set together with different pile diameters (Dp) equals 0.8, 1.27 and 2.5 centimeters and different distances from the abutment nose to piles (x) equals 2.5, 3.5 and 6 centimeters to study the effect of piles existence on the scour depth. All details are illustrated in fig. (8).

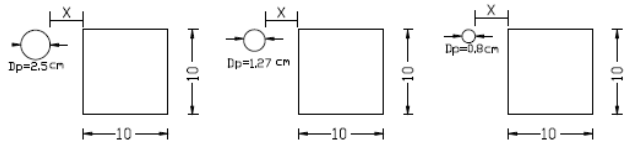

Fig. (8) Plan of the fifth set model

3 DIMENSIONAL ANALYSIS AND REGRESSION

Dimensional analysis is a mathematical method which is used to deduce a homogenous relation, the scour depth (ds) is a function of the following parameters as shown in (1)

$$ds = f\{L_a, B, V, y, \upsilon, \rho, \rho_s, \mu, g, d_{50}, \sigma_g, R, \alpha, \theta, X, D_p\} \quad (1)$$

Where; ds is the maximum scour depth, L_a is the abutment length, B is the abutment width, y is the water depth V is the mean flow velocity, υ is fluid kinematic viscosity, ρ is fluid density, ρ_s is sediment density, μ is dynamic viscosity of fluid, g is the gravitational acceleration, d_{50} is the median diameter of sediment, σ_g is the geometric standard deviation of sediment size distribution, R is the radius of curvature, α is the side slope angel, θ is the internal angel, X is the distance between the abutment and the pile, D_p is the pile diameter.

By using, the Buckingham's π theorem to obtain a new dimensionless functional relationship can be written as follows:

$$ds/y = f\{F_r, \mathrm{Re}, d_{50}/y, L/y, B/y, R/y, \alpha, \theta, X/y, D_p/y\} \quad (2)$$

After eliminating of the constant parameters, the final relation can be written as:

$$ds/y = f\{F_r, R/y, \alpha, \theta, X/y, D_p/y\} \quad (3)$$

Scour phenomena was studied around various models of abutments to develop relations for predicting the scour depth. Four empirical relations were derived using nonlinear regression program SPSS for estimating the maximum relative scour depth around various models of abutments. To check the accuracy of these relations, the statistical performance indicators were used as coefficient of determination (R^2), mean absolute error (MAE), mean absolute percent errors (MAPE) and root mean square error (RMSE). These indicators were defined by [13] as:

$$MAE = \frac{1}{N}\sum_{i=1}^{N}|Yi - Yi`| \quad (4)$$

$$MAPE = \frac{100}{N}\sum_{i=1}^{N}\frac{|Yi - Yi`|}{|Yi|} \quad (5)$$

$$RMSE = \sqrt{\frac{\sum_{i=1}^{i=N}(Yi - Yi`)}{N}} \quad (6)$$

Where; Y_i is the observed value, Y_i` is the corresponding predicted values and N is the total numbers of observed values.

International Journal of Scientific & Engineering Research, Volume 10, Issue 8, August-2019
ISSN 2229-5518

4 RESULTS AND ANALYSIS

4.1 The influence of changing the abutment width on scour depth for vertical abutments

The change of abutment width affects slightly on the maximum scour depth for all applied Froude numbers as illustrated from Fig. (9a) to Fig. (11c).

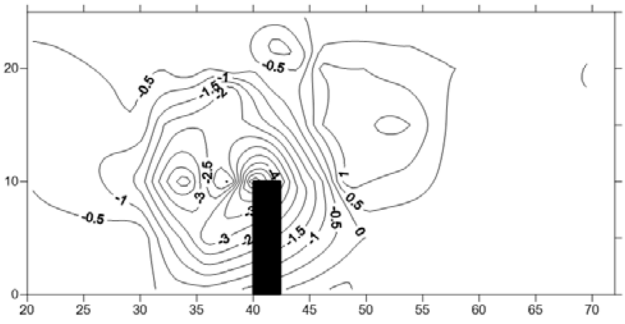

Fig. (9a) Bed contour map around the vertical abutment (B=3 cm) at Fr=0.26

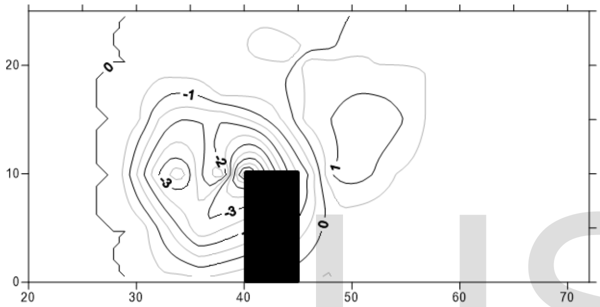

Fig. (9b) Bed contour map around the vertical abutment (B=5 cm) at Fr=0.26

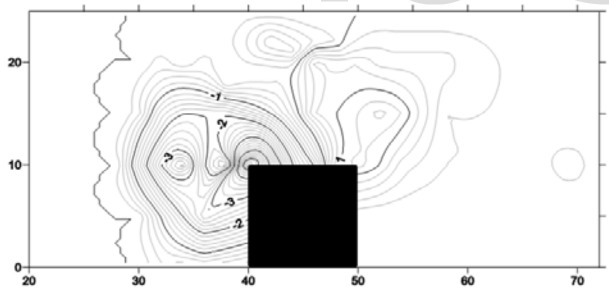

Fig. (9c) Bed contour map around the vertical abutment (B=10 cm) at Fr=0.26

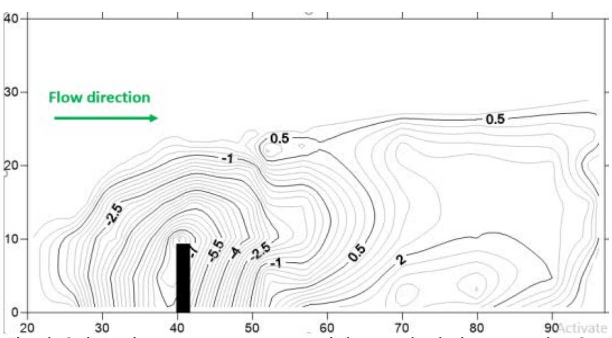

Fig. (10a) Bed contour map around the vertical abutment (B=3 cm) at Fr=0.33

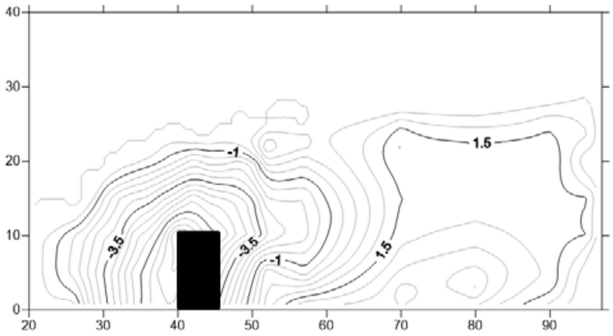

Fig. (10b) Bed contour map around the vertical abutment (B=5 cm) at Fr=0.33

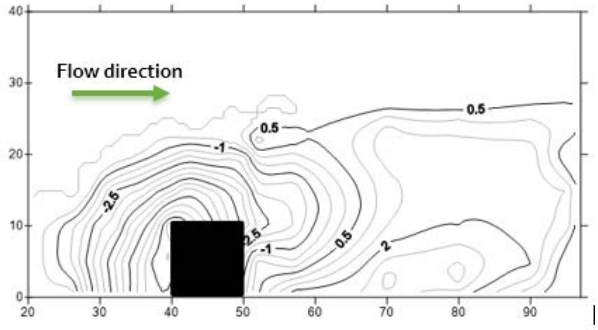

Fig. (10c) Bed contour map around the vertical abutment (B=10 cm) at Fr=0.33

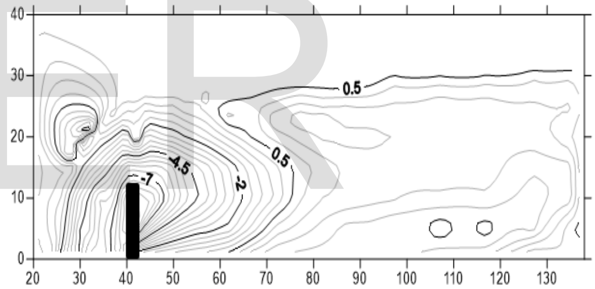

Fig. (11a) Bed contour map around the vertical abutment (B=3 cm) at Fr=0.37

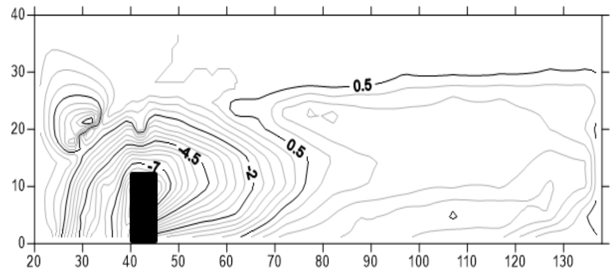

Fig. (11b) Bed contour map around the vertical abutment (B=5 cm) at Fr=0.37

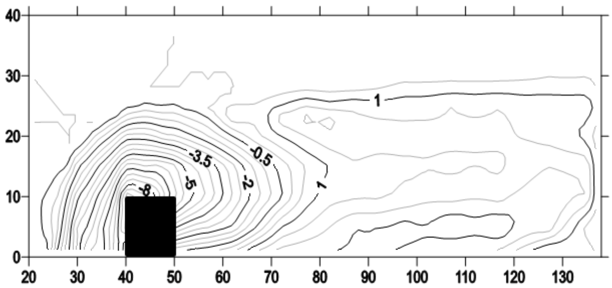

Fig. (11c) Bed contour map around the vertical abutment (B=10 cm) at Fr=0.37

Figure (12) represented the relationship between different Froude numbers and the relative scour depth for studied abutment widths

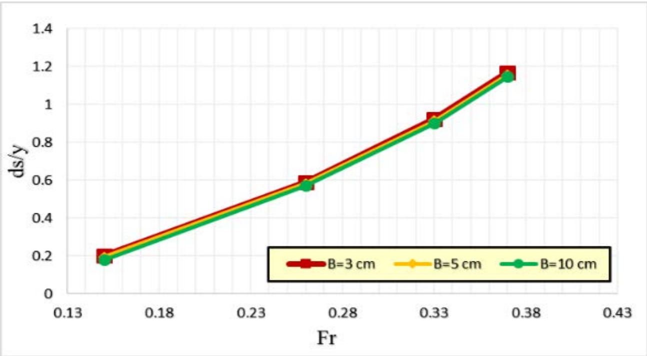

Fig. (12) Relationship between Fr and relative scour depth (ds/y) for studied vertical abutment.

4.1.1 The influence of Froude number on scour depth around vertical abutments

The typical scour hole profile and sediment deposit were clarified in Fig. (13) to study the effect of Froude number on scour depth for vertical abutment with B=10 cm. The negative values in y direction referred to the scour depth and the positive values referred to the sedimentation. It was observed that the scour depth increased as Froude number increased. The largest value of scour depth was located at the abutment nose as shown in Fig. (13).

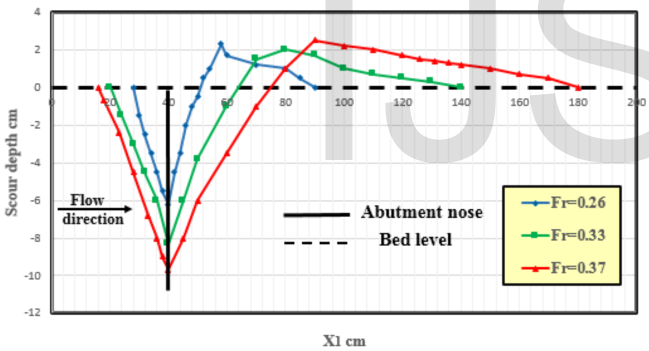

Fig. (13) The influence of Froude number on scour depth around vertical abutment with B=10cm.

4.2 The influence of radius of curvature (*R*) and Froude number on scour depth around semicircular ended abutments

The influence of Froude number variation on local scour around semicircular ended abutments was studied for three radius of curvature (R=1,2 and 3 cm) as illustrated from Fig. (14) to Fig. (16). It was observed that when the Froude number increases, the scour depth increases. The maximum scour depth occurred at the abutment nose for all Froude numbers. The following figures indicate that the increase of curvature radius decrease the scour depth for all applied Froude numbers.

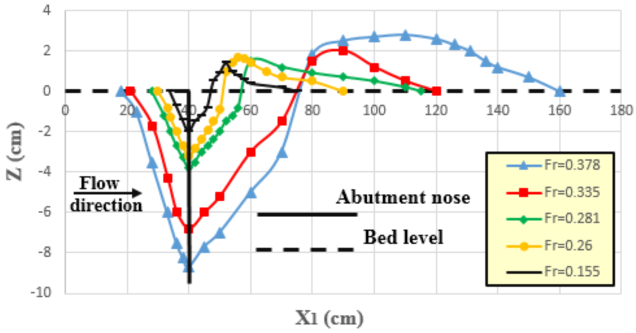

Fig. (14) Cross section elevation of scour around semicircular ended abutment with R=1 cm

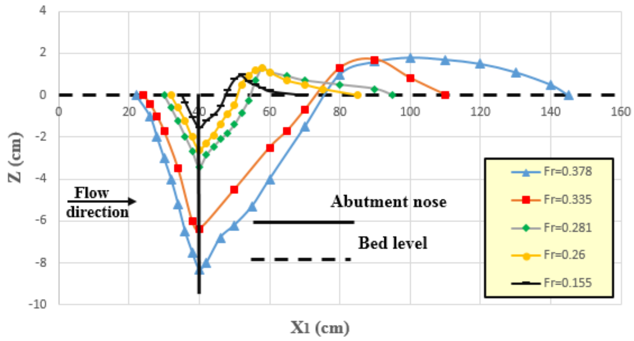

Fig. (15) Cross section elevation of scour around semicircular ended abutment with R=2 cm

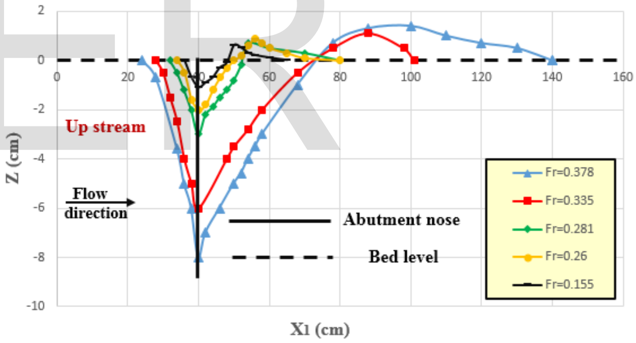

Fig. (16) Cross section elevation of scour around semicircular ended abutment with R=3 cm

4.2.1 The empirical relation for semicircular-ended abutments

Using dimensional analysis and nonlinear regression program SPSS, the relation of relative scour depth of semicircular ended abutments set was obtained and illustrated in table (1). Also, the statistical performance indicators to check the accuracy of this relation are illustrated in the upcoming table.

Table (1)

The relative scour depth relation around semicircular abutment and its performance indicators.

Abutment shape	Relative Scour depth relation	R^2	MAE	RMSE	MAPE
Semicircular ended	$ds/y=26.041(Fr)^{3.486}(R/y)^{-0.082}$ (7)	0.98	0.048	0.22	19.905

Figure (17) indicates a good agreement between measured and estimated values of relative scour depth using Eqn. (7) for semicircular ended abutment.

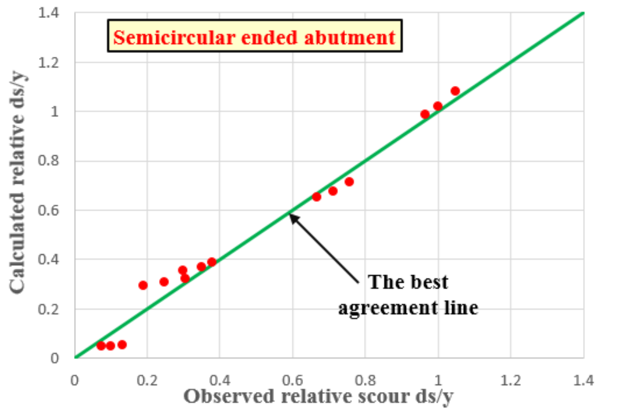

Fig. (17) Comparison between estimated values and experimental results for semicircular ended abutment using Eqn. (7).

Figure (18) illustrates the effect of Froude number on the maximum relative scour depth for semicircular ended abutment using Eqn. (7).

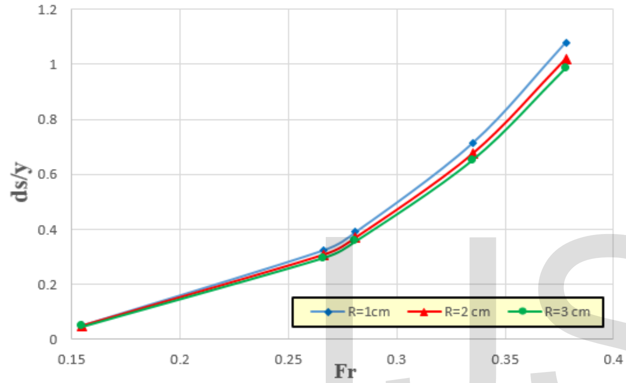

Fig. (18) Variations of relative scour depth versus Froude number for the different models of the semicircular ended abutments using Eqn. (7).

4.3 The influence of side slope angel (θ) and Froude number on scour depth around sloped face abutments

To study The influence of side slope angles (θ) on scour depth for sloped face abutments, Three side slope angles were applied as 20, 15 and 10 degrees. Scour hole profiles are illustrated for different Froude numbers from Fig. (19) to Fig. (21). These figures indicate that the increase of the side slope angel leads to reduce the scour depth for all applied Froude numbers. Also, it was observed that increasing of Froude number leads to increasing the scour depth. The side slope angel of 20 degrees gave the minimum scour depth compared with the other two side slope angels due to the reduction of the abutment's projected area.

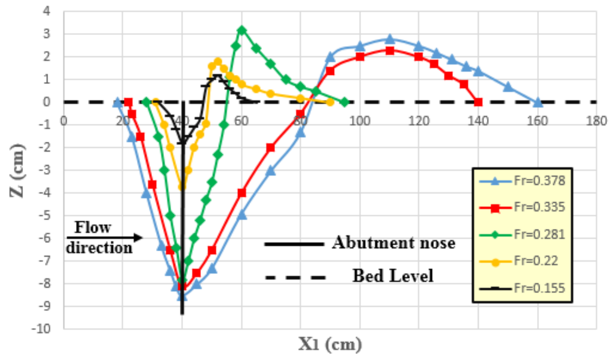

Fig. (19) Cross section elevation of scour around sloped face abutment with $\theta = 10°$

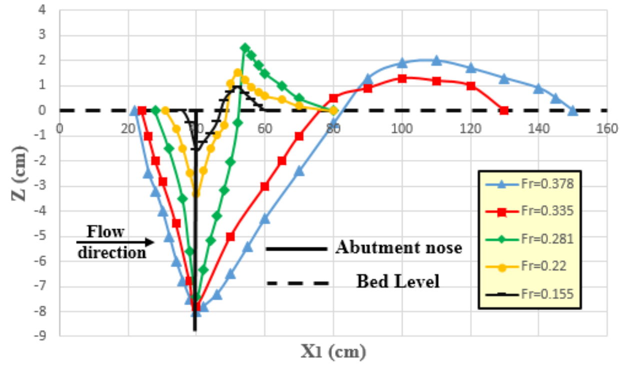

Fig. (20) Cross section elevation of scour around sloped face abutment with $\theta = 15°$

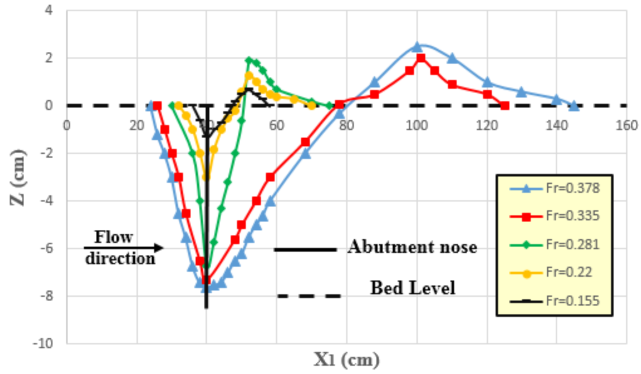

Fig. (21) Cross section elevation of scour around sloped face abutment with $\theta = 20°$

4.3.1 The empirical relation for sloped face abutment

Using dimensional analysis and nonlinear regression program SPSS, the relation of relative scour depth of sloped face abutments set was obtained and illustrated in table (2). Also, the statistical performance indicators to check the accuracy of this relation are illustrated in the following table.

Table (2)

The relative scour depth relation around sloped face abutment and its performance indicators.

Abutment shape	Relative scour depth relation	R^2	MAE	RMSE	MAPE
sloped face abutment	$ds/y=8.04448\,(Fr)^{2.282}(\theta)^{-0.135}$ (8)	0.97	0.083	0.28	18.489

Figure (22) indicates a good agreement between measured and estimated values of relative scour depth for sloped face abutment using Eqn. (8).

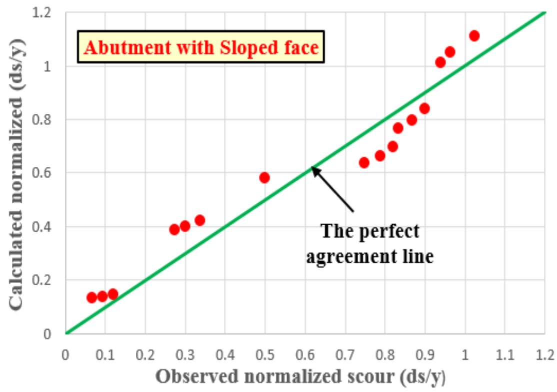

Fig. (22) Comparison between estimated values and experimental results for sloped face abutment using Eqn. (8)

Figure (23) illustrates the effect of Froude number on the maximum relative scour depth for sloped face abutment.

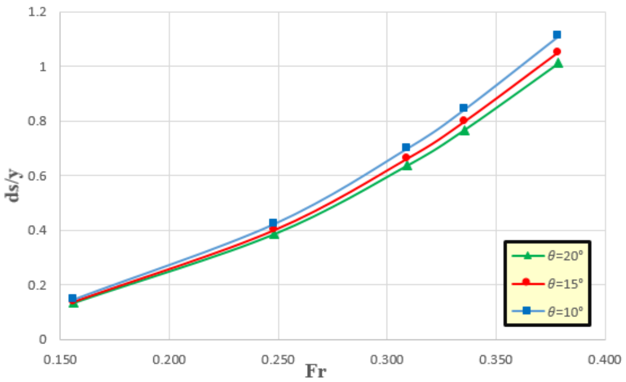

Fig. (23) Variations of relative scour depth versus Froude number. for the different models of the sloped face abutment using Eqn. (8).

4.4 The influence of wall angles (∝) and Froude number on scour depth around wing wall abutments

Wing wall abutments were studied using four angles 60, 65,70 and 90 degrees. Scour hole profiles were illustrated from Fig. (24) to Fig. (27) for different Froude numbers. It was proved that the decrease of the wall angel (∝) leads to reduce the scour depth for all studied Froude numbers. Results showed that the angel of 60 degrees caused the minimum scour depth compared with the other three angels. It minimized the scour depth by 22.68% compared with the developed scour around vertical wall abutment.

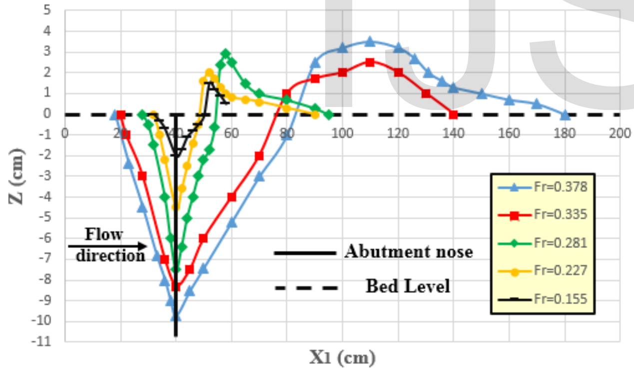

Fig. (24) Cross section elevation of scour around wing wall abutment with (∝) = 90°

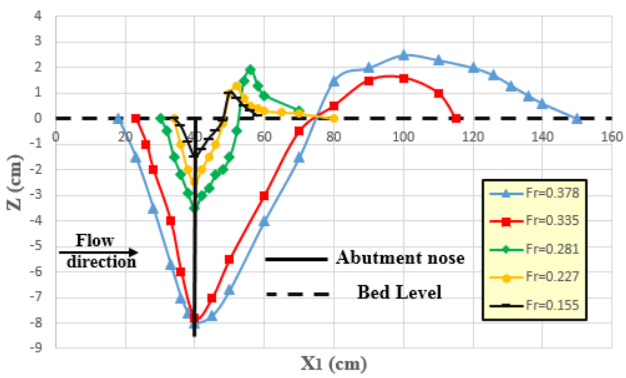

Fig. (25) Cross section elevation of scour around wing wall abutment with (∝) = 70°

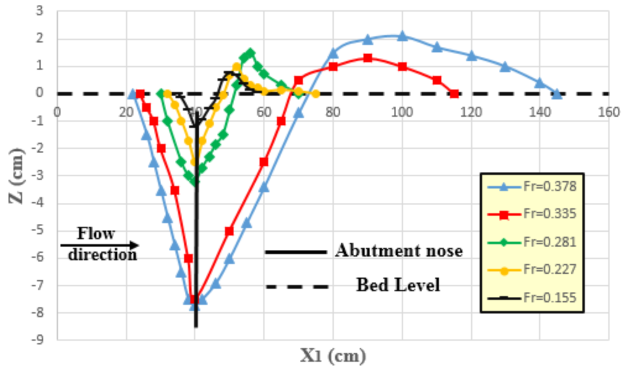

Fig. (26) Cross section elevation of scour around wing wall abutment with (∝) = 65°

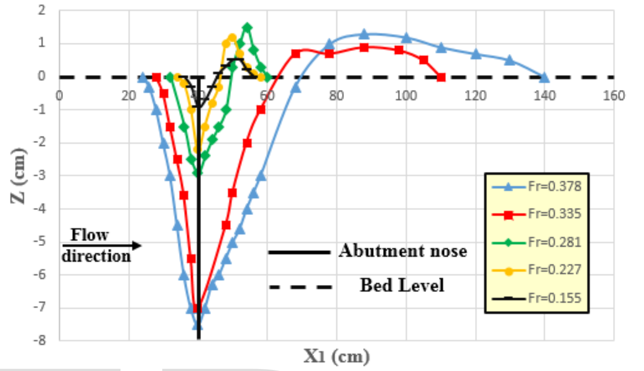

Fig. (27) Cross section elevation of scour around wing wall abutment with (∝) = 60°

Fig. (28) and Fig. (29) indicated that the wing wall abutment with angel 60° resulted in the lowest value for the maximum scour depth compared to the corresponding values of other abutment shapes.

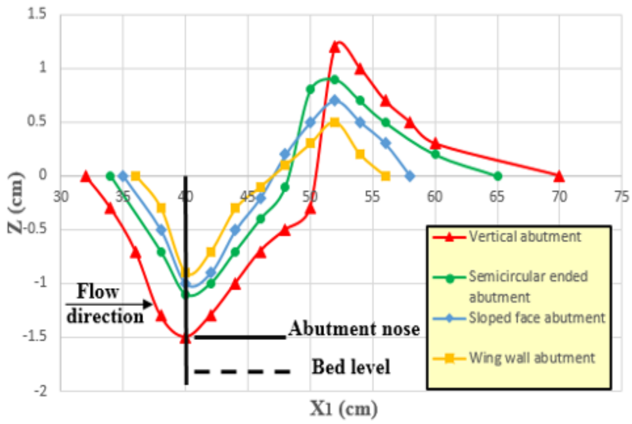

Fig. (28) Cross section elevation of scour different abutment models at Fr=0.155

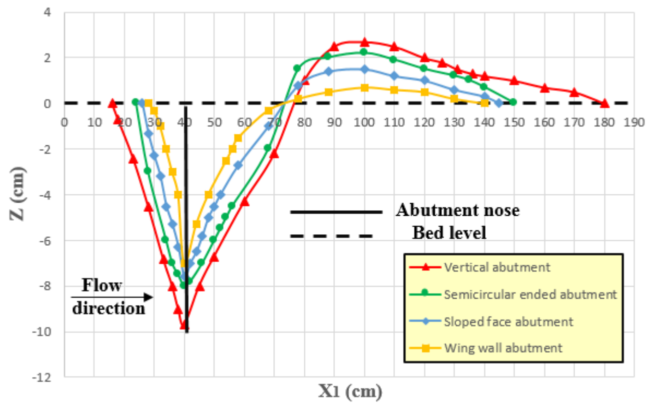

Fig. (29) Cross section elevation of scour different abutment models at Fr=0.379

Fig. (30) and table (3) show the effect of the variation of wall angel (∝) on maximum scour depth relative to the maximum scour depth around wing wall abutment with angle equal to 90 degree (i.e., the vertical abutment). The scour depth reduced as wall angel decreased.

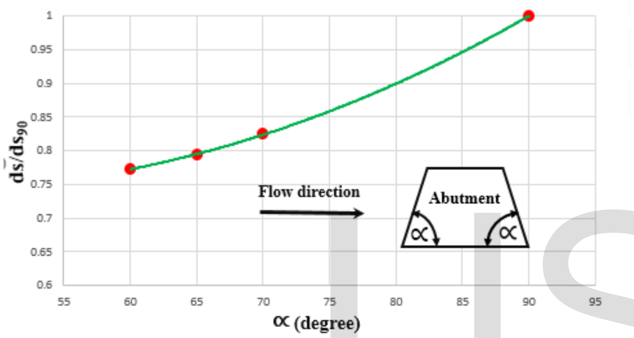

Fig. (30) The influence of wall angel on scour depth.

Table (3)

The influence of wing wall alignment on scour depth.

α (degrees)	ds (cm)	ds/ds_{90} (%)	Reduction (%)
90	9.7	100	0
70	8	82.74	17.26
65	7.7	79.38	20.62
60	7.5	77.32	22.68

4.4.1 The empirical relation for wing wall abutments

Using dimensional analysis and nonlinear regression program SPSS, the relation of relative scour depth is obtained and illustrated in table (4). Also, the statistical performance indicators to check the accuracy of this relation are illustrated in the following table.

Table (4)

The relative scour depth relation around wing wall abutment and its performance indicators

Abutment shape	**Relative scour depth relation**	**R^2**	**MAE**	**RMSE**	**MAPE**
Wing wall abutment	$ds/y=10.84\ (Fr)^{2.509}(\propto)^{0.532}$ (9)	0.96	0.084	0.29	19.483

Figure (31) indicated a good agreement between measured and estimated values of relative scour depth for wing wall abutment Eqn. (9) result.

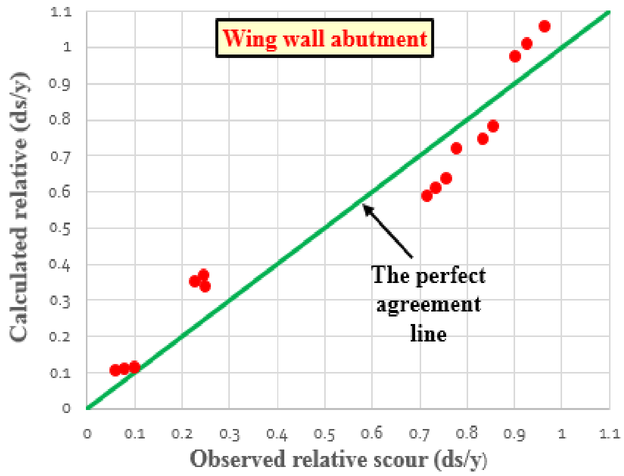

Fig. (31) Comparison between estimated values and experimental results for wing wall abutment using Eqn. (9).

Figure (32) illustrates the effect of Froude number on the maximum relative scour depth for wing wall abutment.

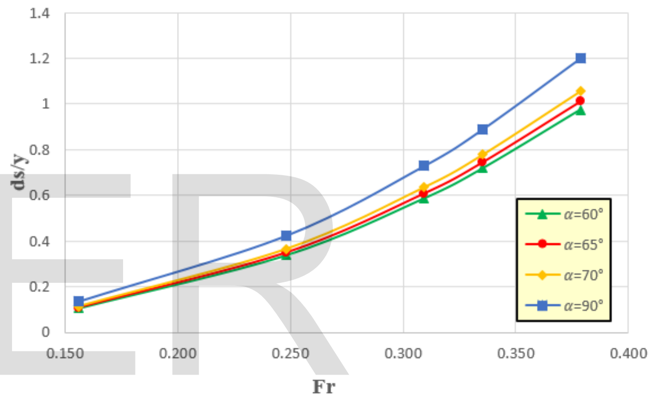

Fig. (32) Variations of relative scour depth versus Froude number. for the different models of wing wall abutment Eqn. (9) result.

4.5 The influence of sacrifice pile on scour depth for vertical abutments

Vertical abutment and Sacrifice piles were used with different pile diameters (D_P) equals 0.8, 1.27 and 2.5 centimeters and different longitudinal distances (x) from the abutment nose to piles site equals 2.5, 3.5 and 6 centimeters. The relation between relative scour depth (ds/y) and the Froude number (Fr) with protective pile and without a protective pile was illustrated from Fig. (33) to Fig. (35). These figures showed that the value of the relative scour depth (ds/y) increased as the Froude number increased. For (D_P/B=0.25), the pile existence had a slight effect on reducing the scour, while the relative pile diameter of (D_P/B=0.08) gave the maximum reduction in both of maximum scour depth and scour volume. Also, results indicated that the relative scour depth decreased to the minimal values in the case of x/B = 0.25 and D_P/B=0.08. This case reduced the maximum scour depth by about 22% and scour volume by about 28% compared with no pile case.

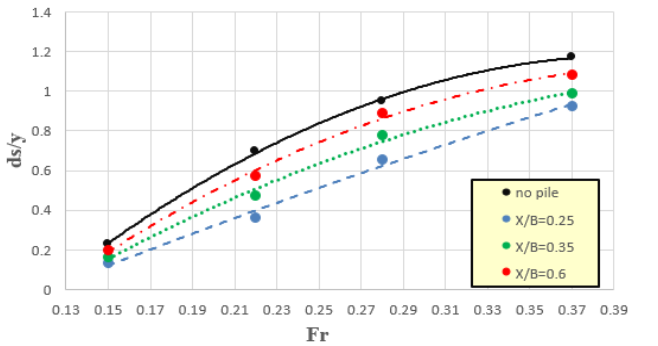

Fig. (33) Variations of relative scour depth versus Froude number (Fr) for pile diameter (D_P/B) = 0.08

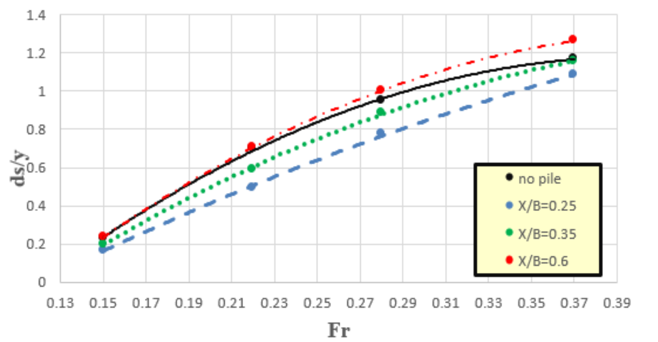

Fig. (34) Variations of relative scour depth versus Froude number (Fr) for pile diameter (D_P/B) = 0.127

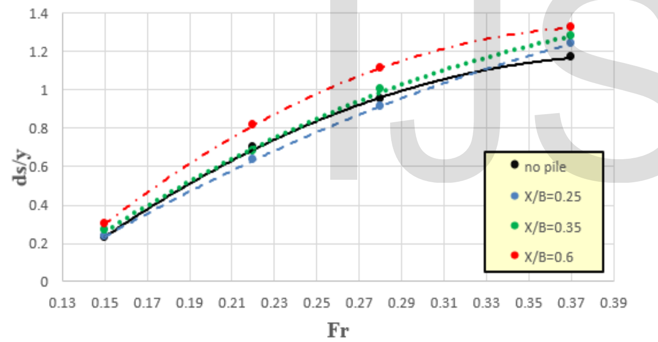

Fig. (35) Variations of relative scour depth versus Froude number (Fr) for pile diameter (D_P/B) = 0.25

4.5.1 The empirical relation for vertical abutment with sacrifice piles

Using dimensional analysis and nonlinear regression program SPSS, the relation of relative scour depth in this set is obtained and illustrated in table (5). Also, the statistical performance indicators are illustrated in the following table to check the accuracy of this relation.

Table (5)

The relative scour depth relation around vertical abutment with sacrifice pile and its performance indicators

Abutment shape	Relative scour depth relation	R^2	MAE	RMSE	MAPE
vertical abutment with sacrifice pile	$ds/y=7.0495\ (Fr)^{1.177}(D_P/y)^{0.243}(x/y)^{0.231}$ (10)	0.96	0.067	0.26	17.624

Where; D_P/y is the relative pile diameter and x/y is the relative pile position.

Results obtained using relation (10), indicate a good agreement between measured and estimated values of relative scour depth as illustrated in figure (36).

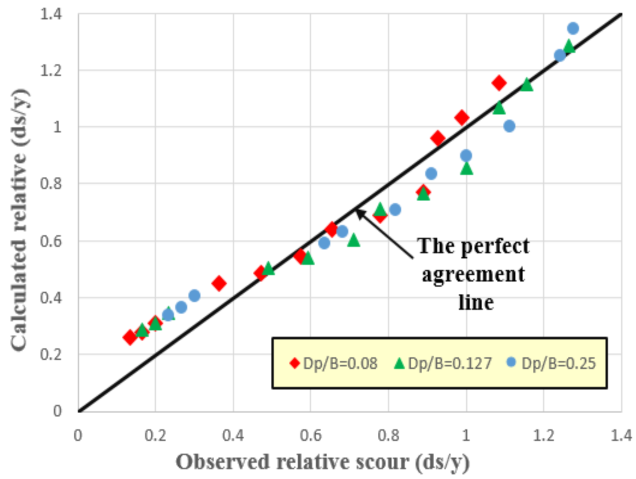

Fig. (36) Comparison between predicted values and experimental results for vertical abutment with sacrifice piles using Eqn. (10).

Figure (37) illustrate the effect of Froude number on the maximum relative scour depth for vertical abutment with sacrifice piles.

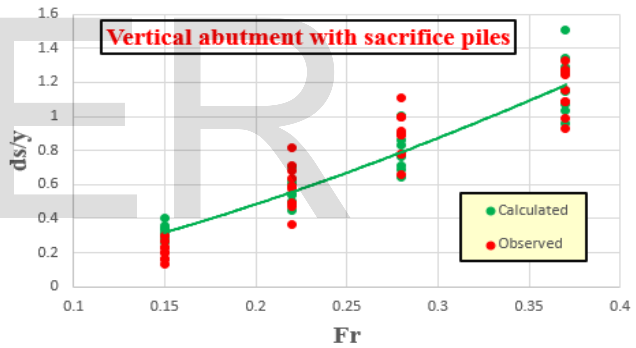

Fig. (37) Comparison between predicted values and experimental results for vertical abutment with sacrifice piles using Eqn. (10).

To show the ability of the developed relation and its performance in predicting the maximum scour depth around vertical abutment with pile existence, relation proposed by [14] was used. This relation was written as **h_s/y=3.574 Fr-0.053 D/y-0.003 x/y-0.004 b/y-0.154** where; **h_s/y** is the relative scour depth and **b** is the abutment width.

Minimum percentage of error 25% was used to check the accuracy of relations, this range of measuring error is acceptable in many hydraulic researches such as [15], [16].

The proposed empirical relation show good agreement range compared with Elnikhely relation as illustrated in Fig. (38).

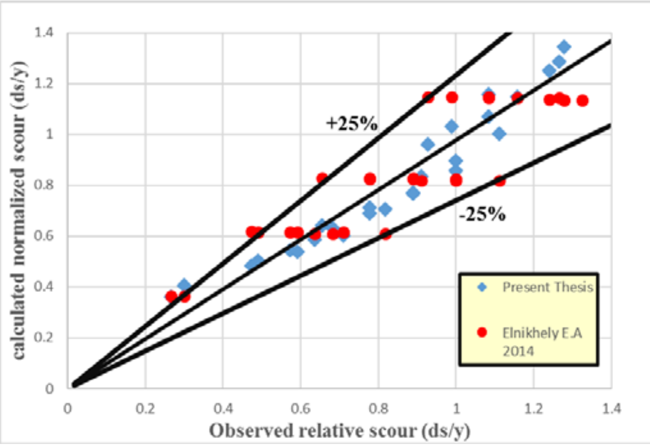

Fig. (38) Comparison between calculated and observed relative scour depths using Eqn. (10) with Elnikhely E. A. 2014.

5 CONCLUSIONS

Experimental study was carried out to investigate the local scour depth around bridge abutments for the proposed shapes. Also, the influence of sacrifice pile existence on the maximum scour depth was studied in this research. During runs it was observed that the scour process started at the intersection of upstream face and the abutment front part. Meanwhile, the conclusions of this research can be summarized as follows:

- The increase of the radius of curvature in the semi-circular ended abutment decreased the maximum scour depth.
- In case of the abutment with vertical sloped face, the increase of side slope angel (θ) leads to reduce the maximum scour depth.
- For wing wall abutment, it was proved that the decrease of wall angel (∝) reduced the maximum scour depth.
- Wing wall abutment with ∝= 60° gave the minimum scour depth compared with other studied abutment models. It has been reduced the scour depth by 22.68% compared with the developed scour around vertical wall abutment.
- Using sacrifice pile with vertical wall abutment ($D_P/B=0.08$, $X/B=0.25$) leads to reduce the maximum scour depth by 22% compared with no pile case.
- The results of the proposed empirical relations showed an acceptable agreement with the experimental measurements.

6 REFERENCES

[1] Jahan, M 2014, 'Effect of suction on local scour around circular bridge piers', MSc Dissertation, Dept. of Civil and Environmental Engineering, University of Windsor.

[2] Setia, B 2008, 'Equilibrium Scour Depth Time', 3rd IASME / WSEAS Int. Conf. on Water RESOURCES, HYDRAULICS & HYDROLOGY, University of Cambridge, Feb. 23-25,2008, UK, pp. 114-117.

[3] Khodabakhshi, A, Saneie, M & Kolahchi, AA 2014, 'Experimental study on effect of slot level on local scour around bridge pier', International Journal of Research in Engineering and Technology, vol. 3, no.2, pp. 103-108.

[4] Zhai, Y 2010, 'Time-dependent scour depth under bridge-submerged flow', MSc Dissertation, Dept. of Civil Engineering, University of Nebraska.

[5] Shrestha, CK 2015, 'Bridge Pier Flow Interaction and Its Effect on the Process of Scouring', PhD Thesis, Sydney University.

[6] Lin, YB, Chang, KC, Lai, JS & Wu, IW 2004, 'Application of optical fiber sensors on local scour monitoring', Proc. IEEE Sensors, Vienna, Austria, pp. 832-835.

[7] Lin, YB, Chang, KC, Lai, JS & Wu, IW 2004, 'Application of optical fiber sensors on local scour monitoring', Proc. IEEE Sensors, Vienna, Austria, pp. 832-835.

[8] El- Alfy, KS 2006, 'Scour and protection at bridge sites in sandy bed channels under steady and unsteady flow conditions', Civil Engineering research magazine, vol. 28, no. 3.

[9] Federal Highway Administration, (2001). Evaluating Scour at Bridges. National Highway Institute, Publication No. FHWA NHI 01-001, HEC No. 18, U. S.

[10] Davari, V 2013, 'Experimental Analysis of Scour Countermeasures at Abutments', MSc Dissertation, Politecnico Di Milano University.

[11] May, R W P, Ackers, J C, & Kirby, A M. (2002) Manual on scour at bridges and other hydraulic structures. London: Construction Industry Research and Information Association (CIRIA)

[12] Chang F M, 1973, A statistical summary of the cause and cost of bridge failures. Office of Research, Federal Highway Administration, Washington D C, US.

[13] Najafzadeh, M., and Gh A. Barani. 2011. "Comparison of Group Method of Data Handling Based Genetic Programming and Back Propagation Systems to Predict Scour Depth around Bridge Piers." Scientia Iranica 18(6): 1207–13

[14] Elnikhely E.A. 2014. "Control of Local Scour at A Bridge Abutment Using a Protective Pile." Journal of Engineering Sciences Assiut University Faculty of Engineering Vol. 42 No. 4.

[15] Wang, Chuan Yi, Han Peng Shih, Jian Hao Hong, and Rajkumar V. Raikar. 2013. "Prediction of Bridge Pier Scour Using Genetic Programming." Journal of Marine Science and Technology (Taiwan) 21(4): 483–92.

[16] Basser, Hossein et al. 2014. "Predicting Optimum Parameters of a Protective Spur Dike Using Soft Computing Methodologies a Comparative Study." Journal Elsevier at science direct Computers and Fluids 97: 168–76.